

Supporting Information

Rational Design of Nanoparticle/Monomer Interfaces: A Combined Computational and Experimental Study of In Situ Polymerization of Silica Based Polymeric Nanocomposites[‡]

§Antonio De Nicola,^{1,2} §Roberto Avolio,³ Francesco Della Monica,¹ Gennaro Gentile,³ Mariacristina
Cocca,³ Carmine Capacchione,¹ Maria Manuela Errico,^{3*} Giuseppe Milano^{1,2*}

¹Dipartimento di Chimica e Biologia and NANOMATES, Research Centre for NANOMaterials
and nanoTEchnology at Università di Salerno, I-84084 via Ponte don Melillo Fisciano (SA), Italy

²IMAST Scarl-Technological District in Polymer and Composite Engineering Scarl Piazza Bovio
22, 80133 (Naples) Italy

³Institute for Polymers, Composites and Biomaterials (IPCB–CNR), Via Campi Flegrei 34, 80078,
Pozzuoli, Italy

§Both of these authors contributed equally to this work.

[‡]Dedicated to the memory of Adolfo Zambelli.

Experimental Section

Materials.

Methylmethacrylate (MMA, 99%, Sigma-Aldrich) was purified from inhibitor by means of a prepacked column for hydroquinone removal (Sigma-Aldrich).

2,2'-Azobis(2-methylpropionitrile) (AIBN, 98%, Sigma-Aldrich) was recrystallized from acetone and dried over P₂O₅ prior to use.

The chain transfer agent (ⁱPr)(H₂O)Co^{III}(dmg-BF₂)₂ was synthesized according to the literature¹.

Dibenzoylperoxide (DBPO, purum, Fluka) and toluene (99.9%, HPLC grade, Sigma-Aldrich) were used without further purification.

PMMA₅, M_n 556 M_w/M_n 1.33; PMMA₇, M_n 696 M_w/M_n 1.23; PMMA₁₆, M_n 1580 M_w/M_n 1.10; were purchased from Agilent Technologies as GPC/SEC standards.

Fumed silica nanoparticles (Aerosil 200, BET surface area 200 ±25 m² g⁻¹, mean diameter of primary particles 12 nm), coded as SiO₂, were kindly supplied by Evonik-Degussa. SiO₂ was heat-treated at 200°C for 24 h before using.

Adsorption of PMMA oligomers onto silica surface.

300 mg of silica nanoparticles were added to 10 mL of toluene solutions prepared dissolving 50 mg of each PMMA_n oligomer. These mixtures were sonicated for 10 min using a Sonics Vibracell ultrasonic processor (500 W, 20 kHz Sonics & Materials, Newtown, CT, USA) at 25% of amplitude. The dispersions were then kept at room temperature under mechanical stirring overnight. After this time, the suspensions were centrifuged to separate the silica rich phases (insoluble fractions). Finally, these phases were repeatedly washed through 5 washing and centrifugation cycles, to remove any non-interacting organic fraction.

Synthesis of MMA_n macromonomers.

MMA_n macromonomers were synthesized according to a procedure reported in literature². Under inert atmosphere AIBN (500 mg; 3.0 mmol) and (ⁱPr)(H₂O)Co^{III}(dmg-BF₂)₂ (74 mg, 0.17 mmol) were dissolved in degassed dry acetone (500 mL). MMA (500 mL; 468 g; 4.67 mol) was added to the solution and the oligomerization was carried out for 4 h at 72 °C. After cooling to room temperature, the solvent and unreacted MMA were removed by rotary evaporation.

Fractional distillation afforded MMA₂, MMA₃ and a MMA₄ rich fraction. Pure MMA₄ was obtained by column chromatography on silica gel (light petroleum ether : ethyl acetate - 4 : 1). Yield MMA₄: 8.19 g, 20 mmol, 0.4%. ¹H- NMR (300.13 MHz, CDCl₃, 25 °C): □ 0.94 (3H, s), 0.97 (3H, s), 1.06 (3H, s), 1.15 (3H, s), 1.90 - 2.20 (4H, m), 2.51 (2H, s), 3.60 (3H, s), 3.64 (3H, s), 3.72 (3H, s), 5.48 (1H, s), 6.20 (1H, s).

Synthesis of poly(methylmethacrylate)-silica nanocomposites.

SiO₂ (1 wt%) was added to a mixture containing MMA and MMA₄ (99 wt%; (MMA)₄/MMA 2.5 mol %). This suspension was sonicated with the above specified ultrasonic processor for 25 min at 25% amplitude using on-off cycles lasting 5 and 30 s, respectively, and cooling the system with an ice bath to prevent that polymerization could start.

Then, the organic peroxide (DBPO, 0.5 wt % with respect to organic fraction) was added to this dispersion to initiate the polymerization reaction. The reaction was performed in two steps: (1) pre-polymerization at 80°C under mechanical stirring until a critical viscosity was reached and (2) the mixture was poured in a glass mould with a 3 mm Teflon spacer sealed on the top surface and kept at 70°C for 18 h in the oven. Then, the temperature was raised at 140°C for 2 h to assure the complete polymerization reaction.

The same experimental procedure was used to prepare material starting from methylmethacrylate monomer (99 wt%) and silica nanoparticles (1 wt%).

After polymerization, to isolate a possible organic interacting fraction, both nanocomposites were dispersed in toluene at room temperature under mechanical stirring overnight. Then, suspensions were centrifuged and the insoluble fractions were repeatedly washed through 5 washing and centrifugation cycles. Silica rich phase recovered from material obtained starting from MMA/MMA₄ mixture was coded as P(MMA-co-MMA₄)-SiO₂. Silica rich phase recovered from material obtained starting from MMA was coded as P(MMA)-SiO₂.

Instrumentations

FTIR spectra were recorded at room temperature by means of a Perkin Elmer Spectrum 100 FTIR spectrometer, equipped with an attenuated total reflectance accessory (ATR). The scanned wavenumber range was 4000–650 cm⁻¹. All spectra were recorded with a resolution of 4 cm⁻¹, and 64 scans were averaged for each sample. The absorption band associated to carbonyl stretching, in the spectral region of 1700-1800 cm⁻¹, was resolved into two components, originating from the bound and free carbonyl fractions, using the Grams/AI 8.0 THERMO Electron Corporation software. A mixed Gaussian-Lorentzian fit was used for both free and hydrogen bonded carbonyls. The relative amount of free- and bound-carbonyl fractions was estimated by the ratio of the corresponding areas.

The adsorbed amount of the organic fraction, (PMMA)_n or (MMA)₄, on SiO₂ was measured using thermogravimetric analysis (TGA) performed on a Perkin Elmer Pyris 1 TGA analyser. Sample of approximately 3-5 mg were placed in a platinum open sample pan and heated from room temperature to 800 °C at 10 °C/min. High purity nitrogen was fluxed through the furnace at a flow

rate of 40 mL/min. In order to account for the silanol condensation of SiO_2 , silica nanoparticles were heated over the same temperature range at the same scan rate. The amount of adsorbed organic phase was obtained by subtracting the silanol weight loss from the total weight loss recorded in the thermograms of $(\text{PMMA})_n\text{-SiO}_2$ or $(\text{MMA})_4\text{-SiO}_2$ sample.

Solid state ^{13}C NMR spectra were collected at 100.5 MHz on a BrukerAvance II 400 spectrometer operating at a static field of 9.4 T, equipped with a 4 mm magic angle spinning (MAS) probe. Samples were finely ground and fit inside 4 mm zirconia rotors sealed with Kel-F caps, then spectra were acquired using a ^1H - ^{13}C cross-polarization (CP) with high power proton decoupling. CP experiments were recorded at 6.3 kHz spinning speed, with a ^1H $\pi/2$ pulse width of 3.8 μs , a contact time of 2 ms and a recycle delay of 4 s.

In figure S1 the spectrum of the interacting fraction coded as $\text{P}(\text{MMA-co-MMA}_4)\text{-SiO}_2$, is reported and compared with the spectrum of PMMA_{16} adsorbed onto silica, $(\text{PMMA}_{16}\text{-SiO}_2)$. The spectrum of $\text{P}(\text{MMA-co-MMA}_4)\text{-SiO}_2$ shows the features typical of PMMA as well as the absence of the signals of unsaturated MMA carbons (129 and 138 ppm). These findings confirmed the formation of an interacting PMMA shell onto silica surface and proved that no unreacted MMA_4 was left.

Moreover, the analysis of $\text{PMMA}_{16}\text{-SiO}_2$ spectrum allowed to assign the signal at 41.5 ppm to terminal OCH_3 carbons. This signal, although with a very low intensity, can be observed also in the spectrum of $\text{P}(\text{MMA-co-MMA}_4)\text{-SiO}_2$; the integration of this peak provided an approximate molecular weight of the adsorbed chains of 8000 Da.

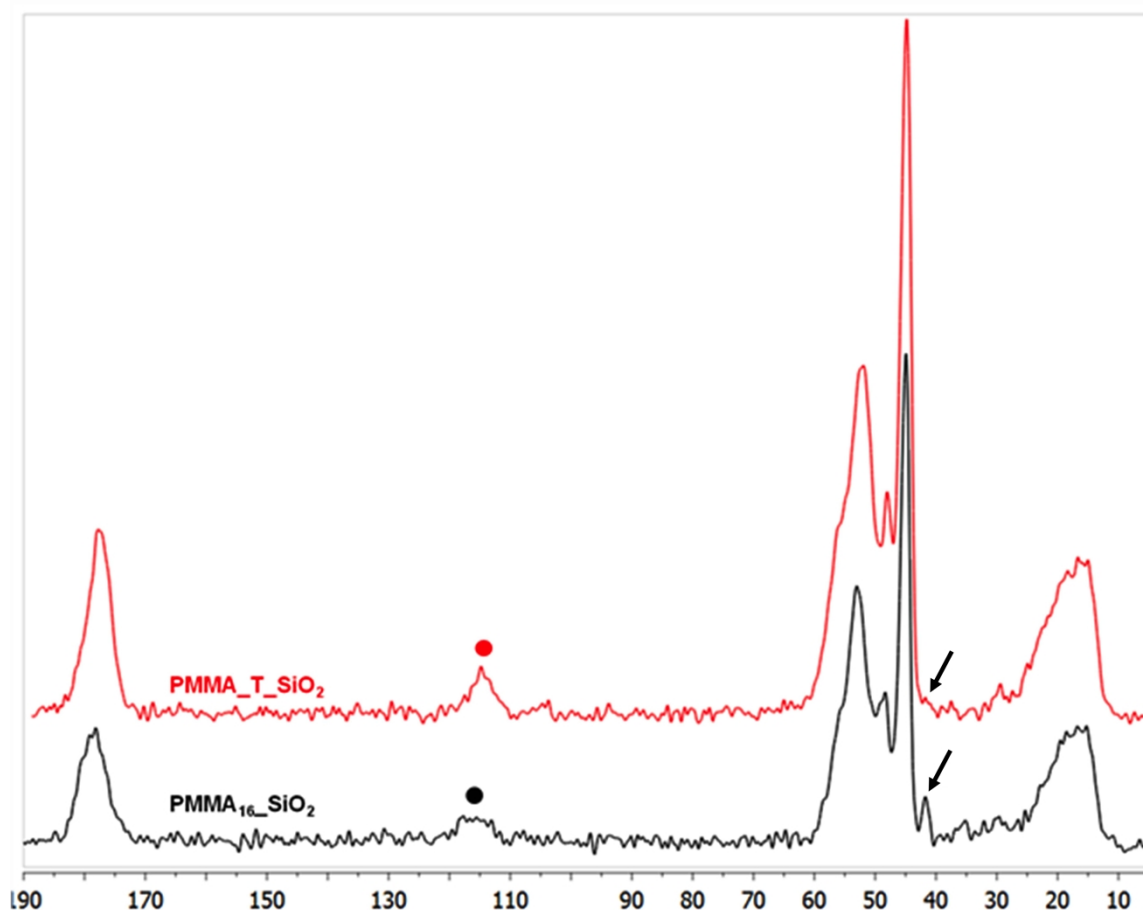


Figure S1. ^{13}C CPMAS spectrum of $\text{P(MMA-co-MMA}_4\text{)-SiO}_2$ and $\text{PMMA}_{16}\text{-SiO}_2$. Signal of terminal carbons are evidenced by arrows, spinning sidebands are marked by a dot.

Bright field transmission electron microscopy (TEM) analysis of nanocomposites was performed on a FEI TECNAI G12 (LaB6 source, 120 kV) microscope equipped with a FEI Eagle 4k CCD camera. Prior to observations, ultramicrotomed sections of the samples were realized and placed on 400 mesh copper grids. In order to determine the average area of the 2D projections (A_{2D}) of the silica agglomerated, image analysis was carried out on a minimum set of 5 TEM micrographs collected at low magnification on different ultramicrotomed sections of each sample.

Computational Section

In this section details about the models of MMA, PMMA and silica nanoparticle are reported.

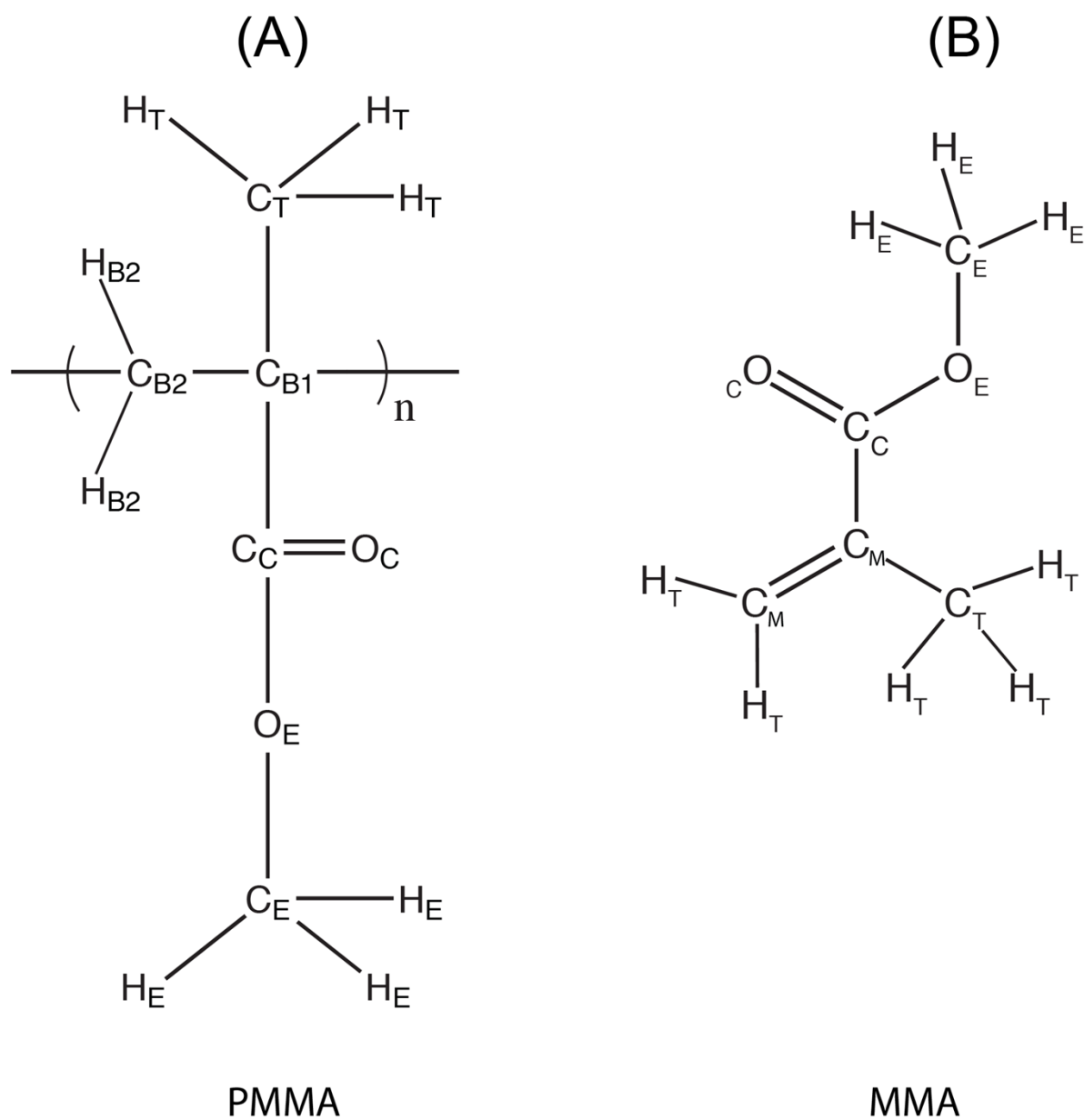


Figure S2: Atom Types for the: A) PMMA and B) MMA model.

Full-Atomistic PMMA Model

The PMMA the model employed in the present study is the one proposed by Maranas³. Below report the functional forms and the parameters of the all-atom PMMA model employed are reported.

Non-Bonded Interactions:

$$u(r_{ij}) = 4\varepsilon \left[\left(\sigma / r \right)^{12} - \left(\sigma / r \right)^6 \right] + \left(\frac{1}{4} \pi \varepsilon_0 \right) \left(\frac{q_i q_j}{r_{ij}} \right) \quad (S1)$$

Tab. S1: Interaction non-bonded terms

Atom Type	σ (Å)	ε (kcal/mol)	q_i
CT	3.52	0.067	-0.135
CB2	3.52	0.067	-0.090
CB1	3.20	0.051	0.000
CC	3.75	0.105	0.510
OC	2.96	0.210	-0.430
OE	3.00	0.170	-0.330
CE	3.50	0.066	0.160
HT	2.50	0.030	0.045
HB2	2.50	0.030	0.045
HE	2.42	0.015	0.030
CM	3.55	0.076	(see fig. S3)
HT (bonded to CM)	2.40	0.014	(see fig. S3)

Bond Interactions:

$$V_{bond} = K_{bond} (r_{ij} - r_{ij}^0)^2 \quad (S2)$$

Tab. S2: Interaction bond terms

Bond Type	K_{bond} (kcal/mol/ Å ²)	r_{ij} (Å)	Bond Type	K_{bond} (kcal/mol/ Å ²)	r_{ij} (Å)
CT-CB1	368.00	1.5390	CC-OE	471.00	1.3600
CB1-CB2	300.00	1.5491	CE-OE	342.00	1.4460
CB1-CC	326.00	1.5170	CT-HT	331.00	1.0900
CC-OC	968.00	1.2290	CE-HE	331.00	1.0900
			CB2-HB2	331.00	1.0900
CM-CM	925.00	1.3400	CM-HT	331.00	1.0900
CM-CC	925.00	1.3400	CM-CT	326.00	1.5100

$$V_{angle} = K_{angle} (\theta_{ijk} - \theta_{ij}^0)^2 \quad (S3)$$

Tab. S3: Interaction angle terms

Angle Type	K_{angle} (kcal/mol/rad ²)	θ (deg)	Angle Type	K_{angle} (kcal/mol/rad ²)	θ (deg)
CB1-CB2-CB1	89.50	113.30	CC-OE-CE	84.80	116.40
CT-CB1-CT	87.90	109.47	HT-CT-CB1	35.00	109.50
CT-CB1-CC	87.90	109.47	HT-CT-HT	35.00	109.50
CB1-CC-OE	74.50	111.40	HB2-CB2-CB1	35.00	109.50
CB1-CC-OC	63.30	125.60	HE-CE-HE	35.00	109.50
OC-CC-OE	126.50	123.00	HE-CE-OE	56.00	110.10
CM-CM-HT	69.96	120.00	CM-CC-OE	139.93	123.00
CM-CT-HT	69.96	117.00	CM-CM-CT	139.93	124.00
CM-CC-OC	159.92	125.30	CM-CM-CC	169.91	120.70

$$V_{\text{torsion}}(\phi_{ijkl}) = V_1(1 + \cos(\phi)) + V_2(1 - \cos(2\phi)) + V_3(1 + \cos(3\phi)) + V_4(1 - \cos(4\phi)) \quad (S4)$$

Tab. S4: Interaction torsional terms

Torsion Type	V1 (kcal/mol)	V2 (kcal/mol)	V3 (kcal/mol)	V4 (kcal/mol)
CT-CB1-CB2-CB1	0.27792	0.00000	0.00000	-0.27792
CB2-CB2-CB2-CB1	0.27792	0.00000	0.00000	-0.27792
CC-CB1-CB2-CB1	0.27792	0.00000	0.00000	-0.27792
CT-CB1-CC-OE	0.80784	0.00000	0.00000	-0.80784
CB2-CB1-CC-OE	0.80784	0.00000	0.00000	-0.80784
CB2-CB1-CC-OC	2.60000	0.05000	-2.55000	0.00000
CT-CB1-CC-OC	2.60000	0.05000	-2.55000	0.00000
CE-OE-CC-CB1	2.02000	-1.0000	-0.70000	-0.32000
CM-CM-CC-OC	-1.15900	5.39100	2.90500	0.00000
HT-CT-CM-CC	0.41441	1.24324	0.00000	-1.65765

$$V_{\text{torsion}}(\phi_{ijkl}) = \frac{1}{2} K (\phi_{ijkl} - \phi_0)^2 \quad (S5)$$

Tab. S5: Interaction improper torsional terms

Torsion Type	ϕ	K (kcal/mol)
HT-CM-CM-CC	0.000	162.40
HT-CM-CM-CT	0.000	162.40
CM-CM-CC-CT	0.000	162.40
CM-CM-CT-HC	0.000	162.40

All atomMMA Model

For the MMA we consider as initial set of parameters the OPLS-AA Force-Field⁴⁻⁵ for the atoms type that differ from the PMMA model of Maranas³. In order to have a model able to reproduce

thermodynamic properties in better agreement with respect to experimental data, a fine-tuning of the initial parameters set have been done.

We decided to tune only non-bonded interaction parameter (σ , ϵ) of C_M atom type (see figure S3 below), and the charges of C_M and the relative bonded hydrogen atoms. All the other parameters, bond and non-bond interactions have been kept identical to the PMMA model of Maranas³. In the Table S5 the values of density and ΔH of vaporization of the MMA models calculated for OPLS-AA/Maranas, optimized force field and the experimental ones are reported. The optimized force field reproduces, a bulk density with an error of about 1%, and a ΔH of vaporization with an error less than 1%. In figure S3 the atom types and charges of the optimized MMA models are reported. In tables from S1 to S5 the non-bond and bond parameters are reported.

Tab. S6: Properties calculation

Property	OPLS-AA ⁴⁻⁵	Optimized	Experimental ⁶
Density (293 K)	0.974 (g/cm ³)	0.955 (g/cm ³)	0.946 (g/cm ³)
$\Delta H_{\text{vapor.}}$ (300 K)	41.628 (kJ/mol)	38.854 (kJ/mol)	38.866 (kJ/mol)

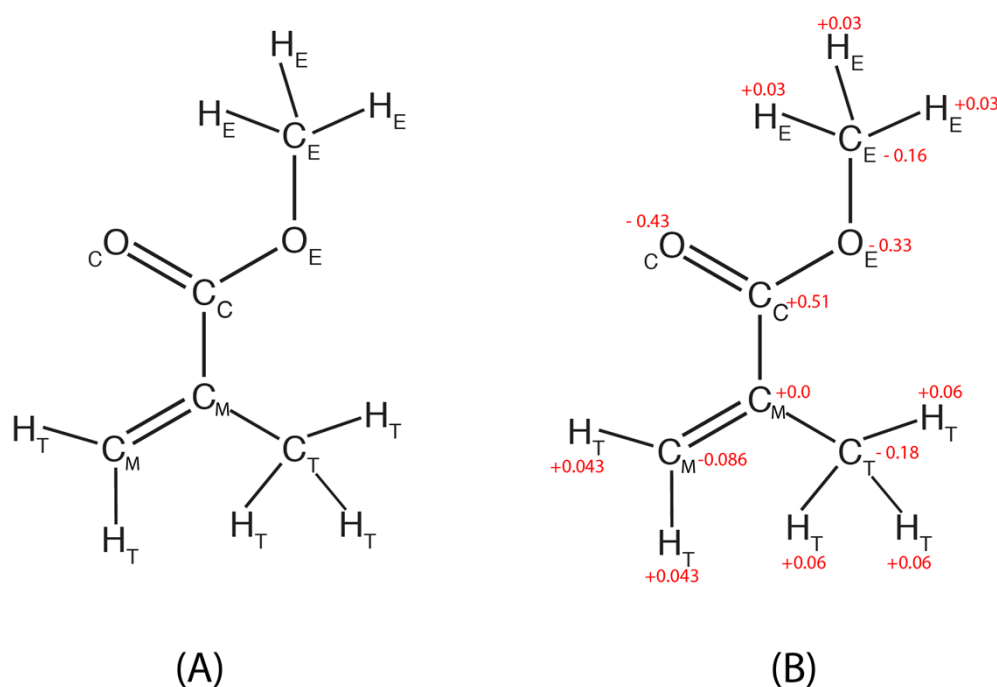


Figure S3: Chemical structure of MMA with atom type (A) and partial charge assignment (B).

Full-Atomistic Silica Nanoparticle

For the silica nanoparticle (NP) we used the model of Brown⁷, that was also employed by Ndoro⁸⁻⁹ and Eslami¹⁰ in studies of interface between silica nanoparticle and polymer matrices. The force field parameters are reported in the table S7 and S8.

Functional form for the non-bonded interactions:

$$u(r_{ij}) = 4\epsilon \left[\left(\frac{\sigma}{r} \right)^{12} - \left(\frac{\sigma}{r} \right)^6 \right] + \left(\frac{1}{4} \pi \epsilon_0 \right) \left(\frac{q_i q_j}{r_{ij}} \right) \quad (S1)$$

Tab. S7: Non bonded

Atom Type	σ (Å)	ϵ (kcal/mol)	q_i
Si	3.154	1.5208	1.020
ON	3.920	0.5997	-0.510
HN	2.352	0.2197	0.255

$$V_{angle} = K_{angle} (\theta_{ijk} - \theta_{ij}^0)^2 \quad (S3)$$

Tab. S8: Bonds

Bond Type	r_{ij} (Å)	Angle Type	K_{angle} (kcal/mol/rad ²)	θ (deg)
Si-ON	1.630	ON-Si-ON	112.18	109.47
ON-HN	0.950	Si-ON-Si	144.00	54.61
		Si-ON-HN	119.52	54.59

The NP have been obtained from a crystal structure of silica α -quartz using the procedure described by Brown⁷ and, in a slightly different but equivalent procedure, by Ndoro⁸⁻⁹. The diameter of NP we used for this study is ~3.0 nm.

Generation of Well-Equilibrated System of Polymer Nanocomposite

Recently De Nicola et al.¹¹ developed a procedure based on molecular dynamics (MD) to generate well-equilibrated system of full atomistic polymer melt, based on soft potential derived from self consistent field (SCF). Such procedure allows obtaining all-atom structures that are indistinguishable from those obtained by usual MD simulations.

The procedure adopted to obtain relaxed, all-atom polymer melt composite is the following:

1. The initial configuration is prepared by placing each chain of PMMA and the silica NP, at random position in the box. The box size has been chosen according to the experimental density of the polymer bulk at the considered temperature.
2. Two different relaxations, using the MD-SCF approach, have been performed. First, the relaxation with χ^*RT interaction parameter have been set to 0.0 for all species. Second, the χ^*RT interaction parameter have been set to 10.00 kJ/mol to all mixing interaction of particles forming different kind of molecules (polymer and NP). The grid size has been kept constant at 0.4 nm for all relaxation procedure.

In the figure S4 the radial distribution functions calculated for the silica NP's c.o.m. respect to the mass center of PMMA chain of full-atomistic MD simulation, MD-SCF ($\chi^*RT=10.0$ kJ/mol) and MD-SCF ($\chi^*RT=0.0$ kJ/mol) are reported.

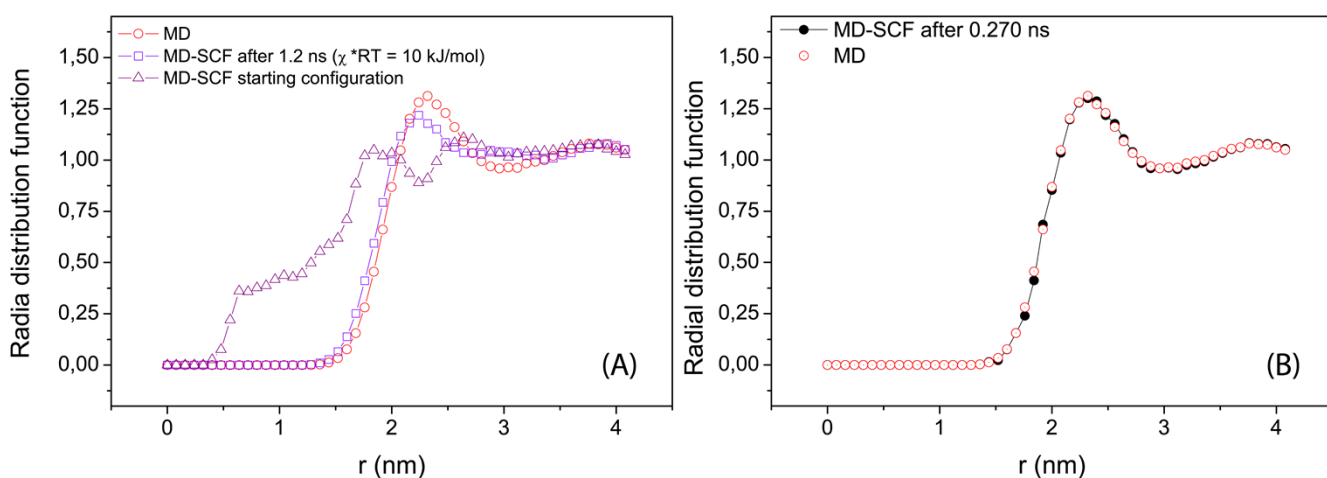


Figure S4:(A) RDF of c.o.m. of silica NP vs. c.o.m. of PMMA chains. (B) Comparison of radial distribution function for full atomistic MD simulation (red circles), MD-SCF configurations after reintroduction of short-range interactions (black circles = 0.270 ns).

Computational Details

The MD-SCF simulations, used to generate the well-equilibrated initial structure of the systems PMMA/silica NP were run in *NVT* ensemble at the temperature of 500 K, controlled by Andersen thermostat¹² (collision frequency 7 ps^{-1}). A time step of 1 fs was employed in all simulations hybrid simulations. The density field was updated every 5 ps. The intramolecular interactions of the hybrid model of PMMA and silica NP used in MD-SCF simulations are identical to those reported in model section.

The MD simulations were carried out in the *NPT* ensemble, a cut-off distance of 1.0 nm was employed for both, van der Waals and Coulomb interactions. The long-range correction to electrostatic interactions were calculated using a reaction-field¹³ with a dielectric constant¹⁴ $\epsilon=2.60$ for PMMA¹⁵ and 3.73 for MMA⁶. The temperature was held constant using Berendsen thermostat¹⁶ ($\tau_T = 0.2 \text{ ps}$), the pressure have been controlled at 1.03 bar using Berendsen barostat ($\tau_P = 2.0 \text{ ps}$) with isotropic coupling. A time step of 2 fs has used for all systems.

Tab. S10: Details of Simulated Systems

Nr.	System	Nr. of Silica NP	Nr. MMA or PMMA	Nr. Rep. unit	Total nr. Particles	Box Length (nm)	Temperature (K)	Time (ns)
1	NP/MMA	1	3981	-	61116	8.77891	353	105
2	NP/MMA	1	3981	-	61116	8.53675	293	112
3	NP/PMMA5	1	757	5	59290	8.28980	500	107
4	NP/PMMA5	1	757	5	59290	8.10097	353	111
5	NP/PMMA5	1	757	5	59290	7.96651	293	132
6	NP/PMMA10	1	385	10	59921	8.22594	500	118
7	NP/PMMA10	1	385	10	59921	8.09921	353	107
8	NP/PMMA10	1	385	10	59921	8.00033	293	109
9	NP/PMMA20	1	196	20	60291	8.92001	500	120
10	NP/PMMA20	1	196	20	60291	8.68830	353	115
11	NP/PMMA20	1	196	20	60291	8.47661	293	120
Systems simulated “in vacuo”								
12	NP/MMA	1	19	-	1364	-	293	110
13	NP/MMA	1	16	-	1313	-	293	85
14	NP/PMMA5	1	78	5	7407	-	293	85
15	NP/PMMA5	1	67	5	6250	-	293	85
16	NP/PMMA10	1	55	10	9871	-	293	85
17	NP/PMMA10	1	49	10	8947	-	293	85
18	NP/PMMA20	1	27	20	9717	-	293	85
19	NP/PMMA20	1	23	20	8485	-	293	85

Additional Results

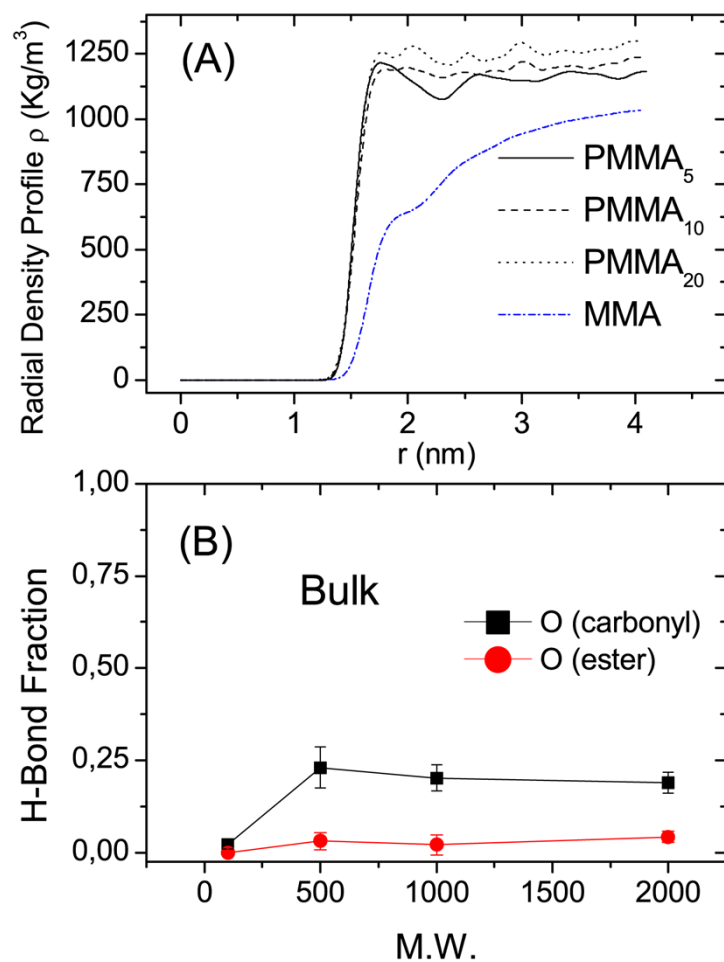


Figure S5: Hydrogen bond fractions calculated as function of molecular weight at 80°C for carbonyl (black curve) and for ester (red curve) oxygen atoms.

Reference:

1. Ram, M. S.; Yap, G. P. A.; Liable-Sands, L.; Rheingold, A. L.; Marchaj, A.; Norton, J. R., Kinetics and Mechanism of Alkyl Transfer from Organocobalt(III) to Nickel(I): Implications for the Synthesis of Acetyl Coenzyme A by CO Dehydrogenase. *Journal of the American Chemical Society* **1997**, *119* (7), 1648-1655.
2. Moad, C. L.; Moad, G.; Rizzardo, E.; Thang, S. H., Chain Transfer Activity of ω -Unsaturated Methyl Methacrylate Oligomers. *Macromolecules* **1996**, *29* (24), 7717-7726.
3. Chen, C.; Maranas, J. K.; Garcia Sakai, V., Local Dynamics of Syndiotactic Poly(methyl methacrylate) Using Molecular Dynamics Simulation. *Macromolecules* **2006**, *39* (26), 9630-9640.
4. Jorgensen, W. L.; Maxwell, D. S.; TiradoRives, J., Development and testing of the OPLS all-atom force field on conformational energetics and properties of organic liquids. *Journal Of The American Chemical Society* **1996**, *118* (45), 11225-11236.
5. McDonald, N. A.; Jorgensen, W. L., Development of an All-Atom Force Field for Heterocycles. Properties of Liquid Pyrrole, Furan, Diazoles, and Oxazoles. *Journal of Physical Chemistry B* **1998**, *102* (41), 8049-8059.
6. David, R. L., Handbook of Chemistry and Physics. CRC Press: 1995.
7. Barbier, D.; Brown, D.; Grillet, A.-C.; Neyertz, S., Interface between End-Functionalized PEO Oligomers and a Silica Nanoparticle Studied by Molecular Dynamics Simulations. *Macromolecules* **2004**, *37* (12), 4695-4710.
8. Ghanbari, A.; Nodoro, T. V. M.; Leroy, F.; Rahimi, M.; Böhm, M. C.; Müller-Plathe, F., Interphase Structure in Silica–Polystyrene Nanocomposites: A Coarse-Grained Molecular Dynamics Study. *Macromolecules* **2011**, *45* (1), 572-584.
9. Nodoro, T. V. M.; Voyiatzis, E.; Ghanbari, A.; Theodorou, D. N.; Böhm, M. C.; Müller-Plathe, F., Interface of Grafted and Ungrafted Silica Nanoparticles with a Polystyrene Matrix: Atomistic Molecular Dynamics Simulations. *Macromolecules* **2011**, *44* (7), 2316-2327.
10. Eslami, H.; Rahimi, M.; Müller-Plathe, F., Molecular Dynamics Simulation of a Silica Nanoparticle in Oligomeric Poly(methyl methacrylate): A Model System for Studying the Interphase Thickness in a Polymer–Nanocomposite via Different Properties. *Macromolecules* **2013**, *46* (21), 8680-8692.
11. De Nicola, A.; Kawakatsu, T.; Milano, G., Generation of Well-Relaxed All-Atom Models of Large Molecular Weight Polymer Melts: A Hybrid Particle-Continuum Approach Based on Particle-Field Molecular Dynamics Simulations. *Journal of Chemical Theory and Computation* **2014**, *10* (12), 5651-5667.
12. Andersen, H. C., Molecular dynamics simulations at constant pressure and/or temperature. *Journal of Chemical Physics* **1980**, *72* (4), 2384-2393.
13. Allen M.P. , T. D., *Computer Simulation of Liquids*. Clarendon Press: Oxford, 1987.
14. Brandrup, J.; Immergut, E. H., *Polymer Handbook*. THIRD EDITION ed.; John Wiley & Sons: New York, 1989.
15. Karol, M., More data about dielectric and electret properties of poly(methyl methacrylate). *Journal of Physics D: Applied Physics* **1997**, *30* (9), 1383.
16. Berendsen, H. J. C.; Postma, J. P. M.; Gunsteren, W. F. v.; DiNola, A.; Haak, J. R., Molecular dynamics with coupling to an external bath. *Journal of Chemical Physics* **1984**, *81* (8), 3684-3690.